Validation of UWM new global ionosphere model during the most severe geomagnetic storm of the year 2018

Paweł Wielgosz, Anna Krypiak-Gregorczyk, Wojciech Jarmołowski, Beata Milanowska, Poland

Key words: GNSS, ionosphere, GIM

SUMMARY

In this contribution, we present a new global ionosphere total electron content (TEC) model developed at UWM in Olsztyn. Our model is based on un-differenced multi-GNSS precise carrier phase data from 260 globally distributed stations and stochastic modeling using the kriging technique. The model performance is evaluated during the most severe geomagnetic storm of 2018, which took place on August 26th. The derived ionospheric TEC estimates are compared to the broadly used global ionosphere model provided by the International GNSS Service (IGS). Our maps are also validated by the self-consistency analysis technique using GNSS data from 23 globally distributed stations. The validation results confirm that the applied stochastic TEC modeling properly reflects variations in the ionospheric TEC induced by the geomagnetic storm. In all cases, our maps present better accuracy than the IGS product.

Validation of UWM new global ionosphere model during the most severe geomagnetic storm of the year 2018

Paweł Wielgosz, Anna Krypiak-Gregorczyk, Wojciech Jarmołowski, Beata Milanowska, Poland

1. INTRODUCTION

The most popular geodetic ionosphere products are the global ionosphere maps (GIMs) provided by the International GNSS Service (IGS). The final IGS maps developed as an official product of the IGS Ionosphere Working Group are the combination of ionosphere products provided by seven Ionosphere-Associated Analysis Centers (IAACs): CASG (Chinese Academy of Sciences), CODG (Center for Orbit Determination in Europe), EMRG (Natural Resources Canada), ESAG (European Space Agency/European Space Operations Centre), JPLG (Jet Propulsion Laboratory), UPCG (Polytechnic University of Catalonia), WHUG (Wuhan University). These GIMs are created by performing a weighted mean of the various IAACs vertical total electron content (VTEC) maps and offer 2.5 by 5.0 degrees spatial resolution, and temporal resolution of 2 h. Unfortunately, according to Hernández-Pajares et al. (2017), their accuracy is in the range from a few total electron content units (TECU) to approximately 10 TECU. It is important to note that each center uses different datasets and modeling techniques to create its own GIM. Consequently, the ionosphere models are characterized by different temporal and spatial resolutions, as well as different accuracy of the VTEC. Taking into account an irregular coverage of the globe by GNSS ground stations, and the occurrence of areas with little or no ground GNSS measurements, it is extremely important to use appropriate estimation or interpolation methods. Studies have shown that the stochastic interpolation methods have some advantages over the deterministic ones (Jarmolowski, 2019). Therefore, in this paper, a new global ionosphere modeling based on precise un-differenced dual-frequency carrier phase data from ground GNSS networks and kriging interpolation is presented. The development of a new global model of the ionosphere was based on the own methodology for the estimation of carrier phase bias present in the carrier phase data. This methodology, presented in Krypiak-Gregorczyk et al. (2017), was already successfully used to provide the highly accurate and high-resolution regional ionospheric TEC maps – see Krypiak-Gregorczyk and Wielgosz (2018). However, in this contribution, we present the application of our method to the global ionosphere mapping.

The accuracy of the new global ionosphere UWM maps – denoted **UWM-gk1-** is verified using one of the most popular evaluation methods – self-consistency analysis (Orús, 2005). The results of the analyzes presented in this paper allow us to state that our developed modeling methodology can also be successfully used for ionosphere modeling on a global scale.

2. METHODOLOGY

The new global ionospheric model **UWM-gk1** was developed at the University of Warmia and Mazury in Olsztyn (UWM). For TEC estimation, we use exclusively precise un-differenced dual-frequency GPS+GLONASS carrier phase data from 260 ground GNSS networks. The data processing is based on a 30-second sampling interval of observations and an elevation cut-off of 10 degrees.

The presented approach to ionosphere modeling is an extension of our regional model to a global one. It consists of a three-step procedure. In the first step, (1) the data processing is based on a geometry-free linear combination (L_{GF}) of dual-frequency carrier-phase observations. This combination eliminates geometry-related observational errors. We use Least Squares Adjustment (LSA) to the estimation of the carrier phase biases for all continuous satellite observation arcs. The accurately estimated carrier phase bias for each continuous data arc is the prerequisite for the resulting accurate ionosphere model. In our global modeling, the ionosphere is parametrized every 20 minutes using spherical harmonics expansion (SHE) of degree and order of 16. In the second step, (2) the precise slant ionospheric delays are calculated by correcting the L_{GF} observables by the estimated carrier phase biases. This results in precise slant ionospheric delays that are subsequently converted into STEC. For slant to vertical TEC mapping at the ionospheric pierce points (IPP) locations, a Modified Single Layer Model (MSLM) mapping function is used. The last step (3) of our global ionosphere modeling uses ordinary kriging (OKR) interpolation of the VTEC data calculated in step (2). Specifically, kriging of point VTEC data at IPPs creates a regular VTEC grid by combining two kriging techniques in two modeling steps: ordinary kriging (OKR) and simple kriging (SKR), see Jarmołowski et al. (2021). This results in our final product – accurate UWM-gk1 GIMs provided with 2.5 by 5.0 degrees spatial and 1-hour temporal resolution, respectively.

3. TEST DATA

The UWM-gk1 model performance is evaluated during the most severe geomagnetic storm of the year 2018, which took place on August 26th (238 DOY) in the low part of the 24th sunspot cycle. This storm is the result of a coronal mass ejection on August 20th, 2018, arriving at Earth and sparking strong G3 class geomagnetic storm conditions. A commonly used measure of magnetic disturbance is the Kp index. It is based on calculations of variations in the horizontal component of the magnetic field and reported in 3-hour periods using a quasi-logarithmic scale. The Kp-index ranges from 0 (very quiet) to 9 (very disturbed). The second important index indicating the severity of a geomagnetic storm is the Dst index. It reaches values near zero during magnetically quiet times and becomes negative as the storm develops. It is assumed that disturbed days are characterized by the Dst index below -50 nT (Joshua et al. 2014).

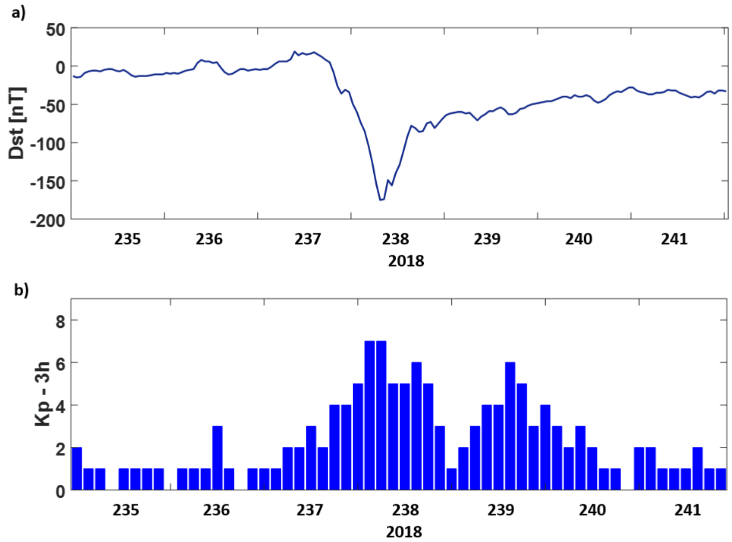

Fig. 1 The variations of the Dst (a) index and the 3-h *Kp* (b) index during the test period - August 23–29, 2018 (DOYs 234-241)

As one can see in Figure 1, the main phase of the storm has begun at 18 UT on August 25th (DOY 237) The Dst index values dropped sharply on August 26th (DOY 238), reaching the minimum of –171 nT at 07.00 UTC and the Kp index reached 7+. In terms of the Dst-index, the analyzed storm is the third strongest of the 24th solar cycle. After the main phase of the geomagnetic storm, which lasted for about 13 hours, there was a slow recovery lasting for a few days.

As was already mentioned, for the modeling we use GNSS data from 260 globally distributed permanent stations. Therefore, in order to validate our global TEC model, additional 23 globally distributed stations were selected (Fig. 2). Note that these stations were not used during the UWM-gk1 model calculation. Moreover, they were not used in the IGS model, which was used here as the reference model. The presented analyses were conducted for seven days from August 23th to 29th, 2018 (DOY 235-241). The test period includes three days before the storm, the main phase of the storm, and three days of the recovery phase (Fig. 1).

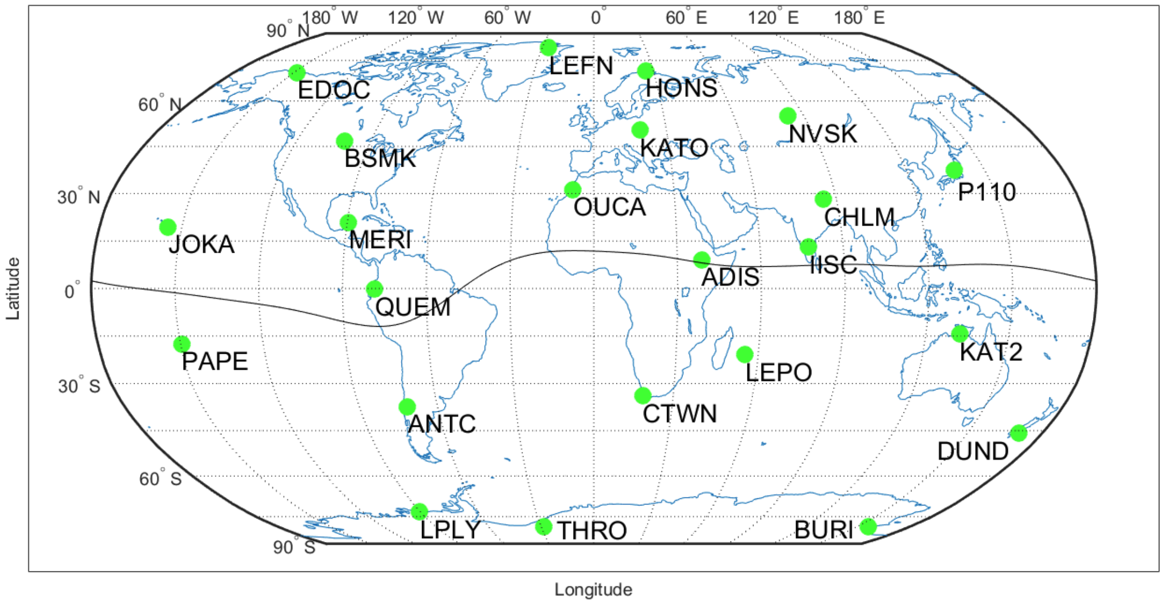

Fig. 3 Distribution of test GNSS-tracking stations used in the self-consistency analysis.

The examples of our TEC maps (GIMs) and the reference IGS GIMs before, during and after the storm are presented in Fig 3. For each of the days, the maps at 18 UT and 8 UT are presented, reflecting the beginning of the disturbance and the peak of the storm, respectively. On DOY 238, a significant increase of the TEC value at 8 UTC was observed for both tested models. A clear evolution from the positive to the negative phase of the storm is visible. On the next day (DOY 239), the ionosphere was in the recovery phase, and the TEC values were still higher than on the quiet day. While at 18 UTC there was a significant increase of the TEC value in relation to the two previous days, especially on the disturbed day. The IGS model has higher TEC values during the three presented days. However, although the spatial resolution of both models is the same, the UWM-gk1 model reflects more details. The accuracy of IGS and UWM-gk1 models will be analyzed in the next section.

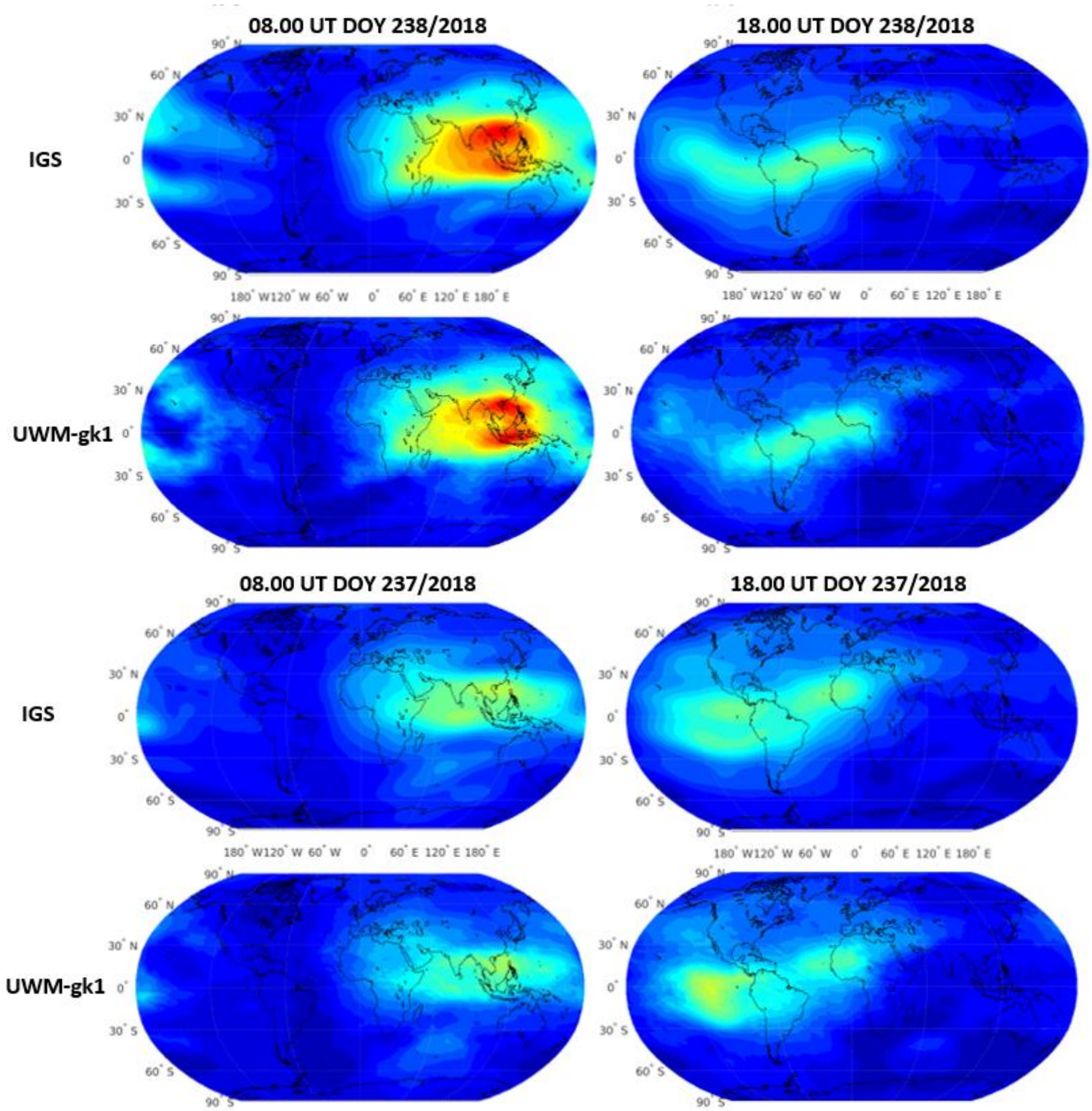
08.00 UT DOY 238/2018
18.00 UT DOY 238/2018
IGS
UWM-gk1
08.00 UT DOY 237/2018
18.00 UT DOY 237/2018
IGS
UWM-gk1

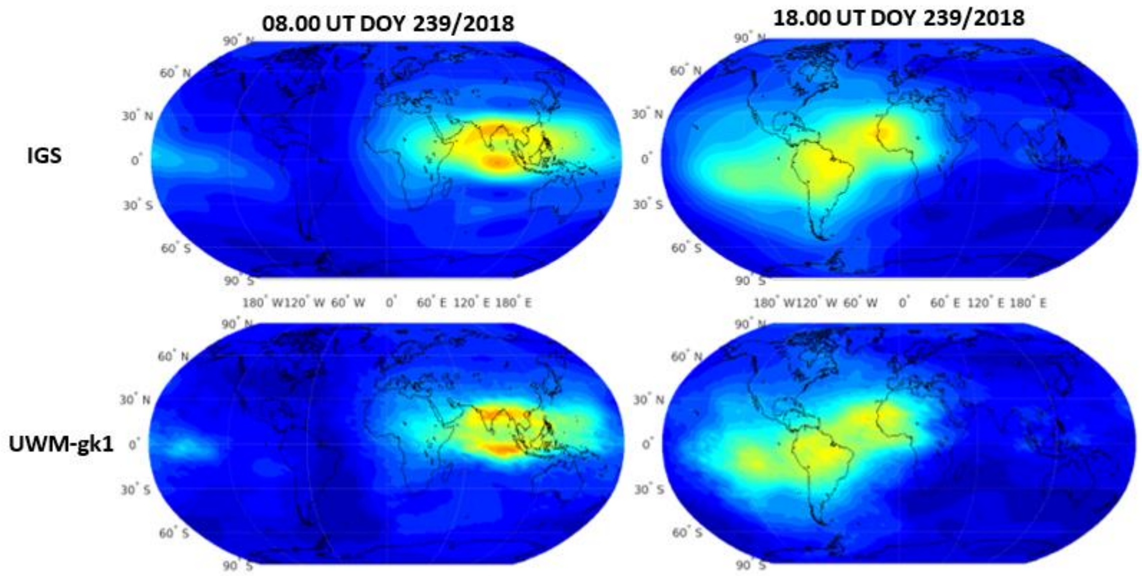

Fig. 3 Example TEC maps derived from UWM-gk1 model and IGS model on a quiet day before the storm (DOY 237), the stormy day (DOY 238), and one day after the storm (DOY 239), at 08.00 UTC (left) and 18.00 UTC (right).

4. SELF-CONSISTENCY ANALYSIS

The validation of UWM-gk1 new global ionosphere maps was based on our own approach for the self-consistency analysis, as presented by Krypiak-Gregorczyk et al. (2017). In this method, UWM-gk1 and IGS GIMs were used independently to calibrate the carrier phase bias (B_{iGF}^{k}) for each continuous carrier phase observational arc. The observation equation is:

$$L_{i\,GF}^{k} = -\xi_{GF}\Delta I_{i}^{k} + B_{i\,GF}^{k} \quad (1)$$

with

$$B_{iGF}^{k} = \lambda_1 N_{i1}^{k} - \lambda_2 N_{i2}^{k} - \left(b_{L1}^{k} - b_{L2}^{k}\right) - \left(b_{L1,i} - b_{L2,i}\right) \quad (2)$$

where $L_{i\,GF}^{k}$ is geometry-free combination of dual-frequency carrier phase signals transmitted by satellite *k* and received by receiver *i*, ΔI_{i}^{k} is ionospheric delay, $B_{i\,GF}^{k}$ is carrier phase bias, and ξ_{GF} is a factor relating the ionospheric delay to *L1* signal. Note that the carrier phase bias consists of differences between the carrier phase ambiguities N_{i1}^{k} *and* N_{i2}^{k}, and also receiver and satellite hardware delays *b* (inter frequency bias) (e.q. 2).

The STEC values determined form L_{GF} observations of GNSS measurements are biased by unknown carrier phase bias that has to be removed by a three-step STEC calibration procedure. Firstly, (1) a geometry-free linear combination of carrier phase observations (L_{GF}) is formed for each continuous data arc. Then, (2) the interpolated VTEC from IGS and UWM-gk1 GIMs for each L_{GF} data arc are converted to STEC values – named GIM_STEC. In this step, we use the interpolation method and the MSLM mapping function presented by Schaer (Schaer et al. 1998, 1999, respectively). Then, (3) the carrier phase bias B_{iGF}^{k} is estimated by fitting carrier phase data (L_{GF}) into GIM_STEC. In the result, we obtain calibrated STEC data, denoted here GNSS_STEC. Based on the post-fit residuals between GNSS_STEC and GIM_STEC, the root-mean-square (RMS) error is calculated. The RMS is used as a GIM accuracy indicator, see for example Wielgosz et al. (2021).

Numerical values of the resulting RMS of the post-fit residuals for the analyzed TEC maps for all test days and stations are presented in Table 1. The daily RMS for the IGS and UWM-gk1 GIMs exceed 1 TECU during the whole test period. However, RMS for IGS GIMs reached as much as 1.91 TECU for the stormy day, while the RMS for the UWM-gk1 maps amounted to 1.62 TECU. After the main phase of the geomagnetic storm, there was a slow recovery for three analyzed days. During the first day of the recovery stage, the level of the RMS of post-fit residuals in the case of the IGS model was higher than during three days before the storm. However, in the case of the UWM-gk1 GIMs its level was the same as during the quiet days. On this day, the difference of the RMS values between the models was the largest (0.34 TECU). The next days of the recovery phase were characterized by a decrease in the RMS of post-fit residuals for both tested models. On the last day, their values dropped to 1.40 TECU for IGS model and 1.11 TECU for the UWM-gk1 model. The difference in the RMS values between the two models reached the same level as for the stormy day (0.29 TECU).

Table 1 RMS of post fit residuals for the analyzed TEC maps. The stormy day is marked with a bold font.

DOY	UWM-gk1 [TECU]	IGS [TECU]	Improvement UWM-gk1 vs. IGS
235	1.13	1.37	+17.5%
236	1.20	1.43	+16.1%
237	1.23	1.50	+18.0%
238	**1.62**	**1.91**	**+15.2%**
239	1.21	1.55	+21.9%
240	1.13	1.43	+21.0%
241	1.11	1.40	+20.7%

Table 2 The overall RMS based on all days and satellite arcs

UWM-gk1 [TECU]	IGS [TECU]	Improvement UWM - gk1 vs. IGS
1.23	1.51	+18.5%

The average RMS based on seven days and satellite arcs for the all tested stations is presented in Table 2. It can be seen that the average RMS for the IGS maps amounted to 1.51 TECU and was 0.28 TECU higher than in the case of the global UWM maps. In general, UWM maps are characterized by lower RMS by18.5%. This confirms that our product based on stochastic VTEC interpolation presents a clear improvement over the official IGS product.

5. CONCLUSIONS

In this contribution, the new global ionosphere model based on processing un-differenced GNSS carrier phase data and kriging interpolation was presented. This model was to provide global ionosphere maps which were analyzed for self-consistency during the most severe geomagnetic storm of 2018. Its results were compared to the reference IGS product. The analysis of the RMS of the post-fit residuals showed that on average the UWM-gk1 maps were characterized by 18.5% lower RMS compared to the IGS one. For the disturbed day, the UWM-gk1 model achieved the RMS values 15.2% lower than the IGS model, while in the recovery phase the advantage of the UWM-gk1 model increased to ~21%.

The UWM-gk1 maps showed slightly the lower TEC level for the disturbed day and the recovery phase, compared to the reference IGS product. At the same time, the UWM-gk1 maps provided a greater level of details of the ionosphere.

In general, it can be stated that our new product based on stochastic VTEC interpolation presents a clear improvement over the official IGS product. Future steps of our global model development will include additional validation by the altimeter data.

Acknowledgments

The study is supported by grant no. UMO-2017/27/B/ST10/02219 from the Polish National Center of Science.

Data Availability Statement:

Products containing ionosphere VTEC maps are accessible from the NASA's CDDIS ftp server (ftp://cddis.nasa.gov/gnss/products/ionex/) in the IONEX format. RINEX files are accessible from the SOPAC (ftp://garner.ucsd.edu/archive/garner/rinex/), UNAVCO (ftp://data-out.unavco.org/pub/rinex/obs/) and SONEL (ftp://ftp.sonel.org/gps/data/) ftp servers. Hourly values of the Dst index were taken from the World Data Center for Geomagnetism at Kyoto University, Japan website (http://wdc.kugi.kyoto-u.ac.jp/dstae/index.html). Kp values were taken from https://ftp.space.dtu.dk/WDC/indices/kp-ap/tab/kp1808.tab.

REFERENCES

Hernández-Pajares M, Roma-Dollase D, Krankowski A, García-Rigo A, Orús-Pérez R (2017) Methodology and consistency of slant and vertical assessments for ionospheric electron content models. J Geod 91(12):1405-1414. DOI: 10.1007/s00190-017-1032-z

Jarmołowski W. (2019) On the relations between signal spectral range and noise variance in least-squares collocation and simple kriging: example of gravity reduced by EGM2008 signal, Bollettino di Geofisica Teorica e Applicata, Vol. 60, Issue 3, p. 457-474, DOI: 10.4430/bgta0265

Jarmołowski W., Ren X., Wielgosz P., Krypiak-Gregorczyk A. (2019) On the advantage of stochastic methods in the modeling of ionospheric total electron content: Southeast Asia case study, Measurement Science and Technology, Vol. 30, Issue 4, 044008, DOI: 10.1088/1361-6501/ab0268

Jarmołowski W., Wielgosz P., Ren X., Krypiak-Gregorczyk A. (2021) On the drawback of local detrending in universal kriging in conditions of heterogeneously spaced regional TEC data, low-order trends and outlier occurrences, Journal of Geodesy, Vol. 95, Issue 1, p. 1-19, DOI:10.1007/s00190-020-01447-8.

Joshua B W, Adeniy J O, Adimula I A, Oladipo O A, Olawepo OA and Adebiyi S J (2014) Ionospheric response to the storm-time disturbance of 29 May, 2010 Advances in Space Research 53 219–225.

Krypiak-Gregorczyk A, Wielgosz P, Borkowski A (2017) Ionosphere model for European region based on multi-GNSS data and TPS interpolation. Remote Sens 9(12):1221. DOI: 10.3390/rs9121221

Orús R (2005) Contributions on the improvement, assessment and application of the Global Ionospheric VTEC Maps computed with GPS data. Ph.D. dissertation. Universitat Politècnica de Catalunya, Barcelona, Spain.

Schaer S, Gurtner W, Feltens J (1998) IONEX: The ionosphere map exchange format version 1. In: Proceedings of the IGS AC workshop, Darmstadt, Germany (Vol. 9, No. 11). IGS Technical Note

Schaer S (1999) Mapping and predicting the Earth's ionosphere using the Global Positioning System. Ph.D. thesis, Ph.D. dissertation. University of Bern, Bern

Wielgosz P., Milanowska B., Krypiak-Gregorczyk A., Jarmołowski W. (2021) Validation of GNSS-derived global ionosphere maps for different solar activity levels: case studies for years 2014 and 2018. GPS Solutions 25, 103. https://doi.org/10.1007/s10291-021-01142-x

BIOGRAPHICAL NOTES

Pawel Wielgosz is a Full Professor at the Department of Geodesy of the University of Warmia and Mazury in Olsztyn, Poland, where he heads a research group on Advanced Methods for GNSS Data Processing. His research interests cover satellite navigation, precise positioning, and GNSS-based ionosphere and troposphere studies. He is the chair of the IAG Sub-Commission 4.4 "GNSS Integrity and Quality Control".

Anna Krypiak-Gregorczyk is an Associate Professor at the Department of Geodesy of the University of Warmia and Mazury in Olsztyn, Poland. Her research interests cover GNSS-based ionosphere studies. She is the chair of IAG JWG 4.3.3 “Validation of VTEC models for high-precision and high-resolution applications”.

Wojciech Jarmołowski is an assistant professor at the Department of Geodesy of the University of Warmia and Mazury in Olsztyn, Poland, where he received his Ph.D. in physical geodesy. His research interests focus on geostatistical modeling of geophysical quantities (gravity, TEC), satellite altimetry, and LEO mission data analysis, as well as GNSS geodetic and geophysical applications.

Beata Milanowska received her master's degree in satellite geodesy in 2019, and is a research assistant at the Department of Geodesy of the University of Warmia and Mazury in Olsztyn, Poland. Her research interests are ionospheric modeling and model evaluation. She is a member of IAG JWG 4.3.3 “Validation of VTEC models for high-precision and high resolution applications”.

CONTACTS

Prof. Paweł Wielgosz
University of Warmia and Mazury in Olsztyn
Oczapowskiego 2
Olsztyn
POLAND
Tel. +
Email: pawel.wielgosz@uwm.edu.pl
Web site: https://www.researchgate.net/profile/Pawel-Wielgosz

Dr. Anna Krypiak-Gregorczyk
University of Warmia and Mazury in Olsztyn
Oczapowskiego 2
Olsztyn
POLAND
Tel. +
Email: a.krypiak-gregorczyk@uwm.edu.pl
Web site:

Dr. Wojciech Jarmołowski
University of Warmia and Mazury in Olsztyn
Oczapowskiego 2
Olsztyn
POLAND
Tel. +
Email: wojciech.jarmolowski@uwm.edu.pl

Web site: https://www.researchgate.net/profile/Wojciech-Jarmolowski

MSc. Beata Milanowska
University of Warmia and Mazury in Olsztyn
Oczapowskiego 2
Olsztyn
POLAND
Tel. +
Email: beata.milanowska@uwm.edu.pl
Web site: https://www.researchgate.net/profile/Beata-Milanowska